



Open Access Articles

The Faculty of Oregon State University has made this article openly available.
Please share how this access benefits you. Your story matters.

Citation	
DOI	
Publisher	
Version	
Terms of Use	

Modification of Rifamycin Polyketide Backbone Leads to Improved Drug Activity Against Rifampicin-Resistant *Mycobacterium tuberculosis**

Aeshna Nigam^{1,§}, Khaled H. Almabruk^{2,§}, Anjali Saxena¹, Jongtae Yang², Udit Mukherjee¹, Hardeep Kaur¹, Puneet Kohli¹, Rashmi Kumari¹, Priya Singh¹, Lev N. Zakharov³, Yogendra Singh⁴, Taifo Mahmud^{2,3} and Rup Lal¹

¹From the Department of Zoology, University of Delhi, Delhi-110007, India

²Department of Pharmaceutical Sciences and ³Department of Chemistry, Oregon State University, Corvallis, OR 97331-3507, U.S.A

⁴Institute of Genomics & Integrative Biology (CSIR-IGIB), Delhi-110007, India

***Running title:** Production of Rifamycin Analogs by *Combinatorial Biosynthesis*

To whom Correspondence would be addressed: Rup Lal, E-mail: ruplal@gmail.com; Taifo Mahmud, Email: taifo.mahmud@oregonstate.edu.

§ These authors contributed equally to this work.

Keywords: Multiple Drug Resistant; Domain Swapping; Polyketide Synthase; Rifamycin analogs; 24-desmethylrifamycin

Background: The emergence of drug resistant tuberculosis has called for the discovery of new antitubercular drugs.

Results: We successfully generated 24-desmethylrifampicin by modifying the rifamycin polyketide backbone.

Conclusion: 24-desmethylrifamycin showed better antibacterial activity than rifampicin against multi-drug resistant strains of *Mycobacterium tuberculosis*.

Significance: The combined genetic-synthetic strategy used in the study has opened up new avenues for generating more rifamycin analogs.

ABSTRACT

Rifamycin B, a product of *Amycolatopsis mediterranei* S699, is the precursor of clinically used antibiotics that are effective against tuberculosis, leprosy and AIDS related mycobacterial infections. However, prolonged usage of these antibiotics has resulted in the emergence of rifamycin resistant strains of *Mycobacterium tuberculosis*. As part of our effort to generate better analogs of rifamycin, we substituted the acyltransferase (AT) domain of module 6 of rifamycin polyketide synthase (*rif*/PKS) with that of module 2 of *rap*amycin

PKS. The resulting mutants (*rifAT6::rapAT2*) of *A. mediterranei* S699 produced new rifamycin analogs, 24-desmethylrifamycin B and 24-desmethylrifamycin SV, which contained modification in the polyketide backbone. 24-desmethylrifamycin B was then converted to 24-desmethylrifamycin S, whose structure was confirmed by MS, NMR, and X-ray crystallography. Subsequently, 24-desmethylrifamycin S was converted to 24-desmethylrifampicin, which showed excellent antibacterial activity against several rifampicin-resistant *M. tuberculosis* strains.

Rifamycin B, a product of the soil bacterium *Amycolatopsis mediterranei* S699, is a clinically important precursor of the broad-spectrum macrolide antibiotics, rifampicin, rifabutin, rifapentine and rifaximin (Fig. 1). Rifampicin, rifabutin, and rifapentine are effective against tuberculosis (TB), leprosy, and AIDS related mycobacterial infections, whereas rifaximin is used to treat enteroaggregative *E. coli* infections. This class of antibiotics binds to bacterial RNA polymerases (RNAPs) and blocks the extension of RNA chain (1,2). However, a long period of use and a combination of poor compliance and poor

medical supervision have resulted in the rifamycin resistant strains of *Mycobacterium tuberculosis*. Therefore, there is an urgent need to produce rifamycin analogs that can overcome this resistance problem. However, structural complexity of rifamycin B limits the use of chemical tools to generate fundamentally different rifamycin analogs, such as modifications of the backbone structure.

Structurally, rifamycin belongs to the ansamycin class of antibiotics, characterized by a naphthalene moiety spanned by an aliphatic chain (Fig. 1). The carbon skeleton of rifamycin B is built by a type I polyketide synthase (PKS) machinery from two acetate and eight propionate units using 3-amino-5-hydroxybenzoic acid (AHBA) as a starter molecule (3). The rifamycin (*rif*) biosynthetic gene cluster (AF040570.3) was first independently identified in *Amycolatopsis mediterranei* S699 (3,4) and LBG A3136 (5), which was then confirmed by genome sequencing of *A. mediterranei* S699 (4) (Fig. 2). The cluster consists of five type I PKS genes, *rifA* to *rifE*, an amide synthase (*rifF*), the AHBA biosynthetic genes, and genes responsible for regulation, efflux, and tailoring processes. The *Rif*-PKS is comprised of a non-ribosomal peptide synthetase-like loading domain (6,7) and ten chain extension modules. Each module consists of a minimal set of domains that includes ketosynthase (KS), responsible for catalyzing a condensation reaction, acyltransferase (AT), which loads the extender unit malonyl-CoA or methylmalonyl-CoA, and an acyl carrier protein (ACP) domain, which tethers the growing polyketide chain. The AT domains of module 2 and 9 recruit malonyl-CoA (incorporating acetate) and the remaining eight modules recruit methylmalonyl-CoA (providing propionate). Additionally, there are modifying domains (ketoreductases, dehydratases, and enoyl reductases) present in the modules. Finally, an amide synthase, *RifF*, is responsible for the polyketide ring closure, leading to an ‘ansa’ structure (8). The genetic organization of the modules in the rifamycin biosynthetic pathway is collinear, similar to the erythromycin (*ery*) and rapamycin (*rap*) PKSs (9,10). This collinear architecture makes it a possible target for combinatorial biosynthesis (11).

Type I PKSs, such as *ery*PKS, have been shown to be amendable to combinatorial

biosynthetic modifications to give new analogs of antibiotics (12-15). For instance, replacement of *debsAT1* and *AT2* with *rapAT14* (16), *debsAT1* with *rapAT2* (13), *debsAT6* with *rapAT2* (17), *debsAT4* with *AT5* domain of nidamycin PKS (18), have resulted in the formation of their respective novel hybrid analogs. Despite these early successes, many attempts to alter PKSs in other systems appeared to be less successful. In the case of rifamycin, ever since the discovery of *rif* PKS, no modifications of this PKS system have been reported. One of the reasons for this is that *A. mediterranei* S699 is less amendable to genetic manipulations. Nevertheless, our early efforts in this direction have resulted in cloning vectors transformation protocol for *A. mediterranei* (19-27). In addition, we have demonstrated that gene manipulations in this strain are possible (28,29). However, whether the *rif*PKS is amendable to genetic manipulations to produce new rifamycin analogs with altered polyketide backbone remains uncertain.

In this paper, we describe for first time the replacement of *AT6* of *rif*PKS (which adds propionate) with *AT2* of rapamycin (*rap*) PKS (which adds acetate to the growing polyketide chain) in *A. mediterranei* S699. The mutant produced 24-desmethylrifamycin B and 24-desmethylrifamycin SV, which were then converted to their semisynthetic derivative 24-desmethylrifamycin S and 24-desmethylrifampicin. These compounds were found to be effective against a number of pathogenic bacteria, including rifampicin-resistant strains of *M. tuberculosis*.

EXPERIMENTAL PROCEDURES

General - All chemicals were obtained either from Sigma Aldrich, EMD, TCI, or Pharmacia. Analytical thin-layer chromatography (TLC) was performed using silica gel plates (60 Å), which were visualized using a UV lamp and ceric ammonium molybdate (CAM) solution. Chromatographic purification of products was performed on silica gel (60 Å, 72–230 mesh). Proton NMR spectra were recorded on Bruker 300, 500, or 700 MHz spectrometers. Proton chemical shifts are reported in ppm (δ) relative to the residual solvent signals as the internal standard (CD₃OD: δ_H 3.35). Multiplicities in the ¹H NMR spectra are described as follows: s = singlet, bs =

broad singlet, d = doublet, bd = broad doublet, t = triplet, bt = broad triplet, q = quartet, m = multiplet; coupling constants are reported in Hz. Carbon NMR spectra were recorded on Bruker 500 or 700 MHz spectrometers. Carbon chemical shifts are reported in ppm (δ) relative to the residual solvent signals as the internal standard. Low-resolution electrospray ionization (ESI) mass spectra were recorded on a Thermo-Finnigan liquid chromatograph-ion trap mass spectrometer. High-resolution mass spectra were recorded on an AB SCIEX TripleTOF™ 5600 equipped with an electrospray ionization source.

Bacterial strains, plasmids, and culture media - *Amycolatopsis mediterranei* S699 (wild-type), a producer of rifamycin B, was obtained from Professor Giancarlo Lancini at the former Lepetit Laboratories, Geranzano, Italy. For sporulation, it was grown at 30 °C on agar plates containing YMG (4 g yeast extract, 10 g malt extract, 4 g glucose, and 15 g agar per liter, pH 7.2-7.4) medium (30). pUC18 and pUC19 were used for subcloning and pMO2 and pIJ4026 were used for domain replacement. *E. coli* XL-1 Blue was used for the propagation and isolation of plasmids. Rifamycin-sensitive and -resistant strains of *Mycobacterium tuberculosis* were acquired from Open Source Drug Discovery (OSDD) (www.osdd.net/) in association with CSIR-Institute of Genomics and Integrative Biology, India (<http://www.igib.res.in/>). The plasmids and bacterial strains that were used in the present study are listed in Supplemental Table S1.

Construction and screening of a genomic cosmid library and selection of the rifamycin cluster - The genomic library of *A. mediterranei* S699 was prepared in the cosmid vector pWE15 (31). This involves isolation of high molecular weight DNA of *A. mediterranei* by Kirby's method (32). The genomic DNA was partially digested with *Sau3AI* and subjected to size fractionation with sucrose gradient. The fractions were pooled and used for ligation with linearized and dephosphorylated pWE15. The ligated DNA was transferred into *E. coli* XL-1 Blue MR. About 2,000 clones were screened using [α -³²P]dATP labeled DNA probes obtained from PCR amplification of the loading domain of *rifPKS* and *rifK* (AHBA synthase gene) of S699. About 10 clones were selected after hybridization. End sequencing of the positive cosmid clones was

performed. Finally, three cosmid clones, pRIF13, pRIF21 and pRIF24, which represent the entire *rif* gene cluster were selected and enlisted in Supplemental Table S1.

Construction of pAT6F - For the construction of the pAT6F replacement cassette, AT6 flanking regions, a 1.6 kb DNA fragment upstream of AT6 (AF040570.3) with engineered *XbaI*/*BalI* sites and a 1.5 kb DNA fragment downstream of AT6 (AF040570.3) with *AvrII*/*XbaI* sites, were obtained by PCR amplification from the cosmid pRIF13. The two amplicons, PCR-I and PCR-II, were treated with kinase and individually cloned into pUC18, which had been digested with *SmaI* at 28 °C and treated with shrimp alkaline phosphatase. The inserts and vector were ligated together and the ligation mix was electroporated into *E. coli* XL-1 Blue competent cells. The constructs containing PCR-I and PCR-II were named pAT6A and pAT6B, respectively. However, due to the cloning of PCR-I in only one orientation, the PCR-I insert was retrieved from pAT6A by digestion with *EcoRI* and *HindIII* and cloned into pUC19, which was predigested with *EcoRI* and *HindIII*. The ligation product was electroporated into *E. coli* XL-1 Blue competent cells. The pUC19 plasmid harboring the PCR-I insert was named pAT6C.

The *rapAT2* (X86780.1) fragment was excised from plasmid pMO2, by *AvrII* and *HindIII* digestion. The resulting 0.85 kb DNA fragment was ligated with *AvrII*/*HindIII*-digested pAT6B to give plasmid pAT6D. Subsequently, the PCR-I fragment was excised from pAT6C by *BalI*/*NdeI* digestion and cloned into the *BalI*/*NdeI* site of pAT6D to give pAT6E. The later plasmid was subsequently digested with *XbaI* to give a 3.85 kb PCR-I/*rapAT2*/PCR-II fragment, which was then inserted into the *XbaI* site of pIJ4026 to give pAT6F (Supplemental Figs. S1-S3). pAT6F was constructed for the implementation of domain replacement (Supplemental Fig. S4) in *A. mediterranei* S699. All clones (pAT6A, pAT6B, pAT6C, pAT6D, pAT6E & pAT6F) were sequenced using the 3100 Avant Genetic Analyzer (Applied Biosystems) at the University of Delhi, India.

Genetic manipulation of A. mediterranei S699 - Routine genetic procedures, such as genomic DNA isolation [according to CTAB (cetyltrimethylammonium bromide) method],

plasmid isolation (Promega DNA purification kit), and restriction endonuclease digestion, were carried out by standard techniques. pAT6F was electroporated (using BioRad GenePulser) into *A. mediterranei* S699 using the method described previously (25), and the electroporated mixture was plated on YMG agar plates, incubated for 12-16 h, and overlaid with soft agar (5 g/L, Difco™ agar, granulated) containing 500 µg/mL of erythromycin. The transformants, obtained after 5-7 days, were grown in YMG medium containing 50 µg/mL erythromycin (Sigma Aldrich) to confirm resistance. The integration of pAT6F in these single crossover (SCO) clones was confirmed by Southern blot hybridization. In order to stimulate replacement of AT6 with *rapAT2*, these SCOs were cultured for 3-4 rounds in YMG medium without erythromycin. The cells were plated on YMG agar plates with and without erythromycin pressure and antibiotic sensitive colonies were selected. The double cross-over (DCO) clones were further confirmed by Southern blot hybridization. For Southern hybridization, the genomic DNA was immobilized on a Hybond N+ membrane (Amersham Biosciences). Hybridization was performed using [α^{32} P]-labeled DNA probes at 65 °C for 12 h. For non-radioactive methods, hybridization was carried out using DIG-labeled DNA probe at 65 °C. Stringency washes were done with 5x SSC, 2x SSC, 1x SSC and 0.1x SSC at 65 °C.

PCR and sequence analysis of the AT6 mutant - Primers were designed based on the sequences of the upstream and downstream regions of *rifAT6* domain of *A. mediterranei* S699, shown in Supplemental Table S2. Chromosomal DNA of the AT6 mutant was isolated using a reported method (32), and PCR amplification was carried out using high fidelity DNA Polymerase (Invitrogen) using conditions and the reaction mix provided with the enzyme. In addition, DMSO (3 µL) was added to the reaction mixture (100 µL). The PCR product (1.5 kb) was confirmed by agarose gel, extracted from the gel using DNA extraction kit (QIAGEN), and submitted to DNA sequencing at the Oregon State University Center for Genome Research and Biocomputing (CGRB).

Isolation and purification of 24-desmethylrifamycin B and 24-desmethylrifamycin SV - Spores of the mutant strain were initially grown on a shaker in YMG medium for 3 days at

30 °C and 200 rpm. The seed culture was then used to inoculate (10%, v/v) YMG medium (10 x 100 mL) in 500 mL flasks. After incubation for 10 days under the same conditions, the cultures were centrifuged, the pooled supernatants acidified to pH 3 with 1N HCl, and the metabolites extracted with ethyl acetate (2 x 1 L). The crude extracts of rifamycin-related compounds were subjected to silica gel chromatography using CHCl₃-MeOH/5%NH₄OH (10:1 and then 8:1) as a mobile phase. Fractions containing the products were pooled and dried using a rotary evaporator. The product obtained was further purified using HPLC [YMC-ODS-A, 250 x 10 mm, CH₃CN-HCOONH₄ (0.05 M) (60:40), flow rate 2 mL/min, 254 nm]. The product was then desalted using Sephadex LH-20 column with MeOH as eluent to give 24-desmethylrifamycin B (20 mg) and 24-desmethylrifamycin SV (8 mg).

24-desmethylrifamycin B: ¹H NMR (700 MHz, D₂O, CryoProbe): δ 6.69 (s, 1H, H-3), 6.34 (d, 1H, *J* = 12 Hz, H-29), 5.98 (d, *J* = 11 Hz, 1H, H-17), 5.75 (dd, *J* = 15 Hz, 11 Hz, 1H, H-18), 5.21 (dd, *J* = 15 Hz, 10 Hz, 1H, H-19), 5.05 (m, 2H, H-25, H-28), 4.50 (d, *J* = 17 Hz, 1H, -CH₂-COOH), 4.42 (d, *J* = 17 Hz, 1H, -CH₂-COOH), 3.38 (bd, *J* = 10 Hz, 1H, H-23), 3.22 (m, 2H, H-21 and H-27), 3.22 (s, 3H, H-37), 2.11 (s, 3H, H-36), 2.08 (s, 3H, H-14), 1.98 (m, 2H, H-20 and H-26), 1.70 (s, 3H, H-13), 1.53 (m, 2H, H-22 and H-24), 1.28 (t, *J* = 12 Hz, 1H, H-24), 0.92 (d, *J* = 6.5 Hz, 3H, H-31), 0.85 (d, *J* = 7 Hz, 3H, H-32), 0.72 (d, *J* = 6.5 Hz, 3H, H-34). ¹³C NMR (175 MHz, D₂O, CryoProbe): δ_C 191.7, 176.7, 174.7, 168.1, 144.7, 142.1, 141.5, 131.5, 126.5, 126.4, 119.4, 117.8, 113.7, 112.8, 112.1, 109.6, 104.4, 101.1, 80.5, 73.9, 72.4, 71.5, 68.8, 54.9, 48.8, 41.4, 39.9, 35.9, 32.2, 21.8, 20.6, 20.5, 15.4, 9.5, 9.5, 6.9. (-)-HR-ESI-TOF-MS *m/z* 740.2939 (calcd for C₃₈H₄₆NO₁₄ [M-H]⁻: 740.2918).

24-Desmethylrifamycin SV: ¹H NMR (700 MHz, CD₃OD, CryoProbe): ¹H NMR (700 MHz, CD₃OD): δ 6.42 (s, 1H), 6.31 (bd, *J* = 12 Hz, 1H), 5.95-5.89 (m, 2H), 5.51 (s, 1H), 5.20 (bt, *J* = 12 Hz, 1H), 5.14 (bd, *J* = 9 Hz, 1H), 3.22 (s, 3H), 3.17 (t, *J* = 10 Hz, 1H), 2.13 (s, 3H), 2.12-2.11 (m, 2H), 2.01 (s, 3H), 1.96 (s, 3H), 1.67 (s, 3H), 1.54-1.49 (m, 4H), 0.93 (d, 6H), 0.78 (d, *J* = 5 Hz, 3H). HRMS (ESI-TOF) *m/z* (calcd for C₃₆H₄₂NO₁₂ [M-H]⁻): 682.2707).

Conversion of 24-desmethylrifamycin B to 24-desmethylrifamycin S - 24-desmethylrifamycin B (8 mg, 0.0107 mmol) was dissolved in MeOH-H₂O (10:1, 5 mL) containing CuCl₂ (0.1 mM). The reaction mixture was stirred at room temperature (RT) overnight to convert 24-desmethylrifamycin B to 24-desmethylrifamycin S. The mixture was acidified to pH 3 and the product was extracted with ethyl acetate (3 x 5 mL). The extract was subjected to silica gel column using CHCl₃-MeOH (10:1) as eluent to give 24-desmethylrifamycin S (6 mg).

¹H NMR (300 MHz, CD₃OD): 7.85 (s, 1H), 7.04 (m, 1H), 6.88 (bd, *J* = 11 Hz, 1H), 6.59 (m, 1H), 5.23 (dd, *J* = 12.6 Hz, 9.7 Hz), 4.53 (bt, *J* = 8 Hz, 1H), 4.22 (bd, *J* = 10 Hz, 1 H), 3.80 (bd, *J* = 10 Hz, 1H), 3.48 (s, 3H), 2.50 (s, 3H), 2.35 (s, 3H), 2.33 (s, 3H), 2.00 (s, 3H), 1.62 (m, 3 H), 1.41 (d, *J* = 7 Hz, 3H), 1.29 (d, *J* = 6.8 Hz, 3H), 0.67 (d, *J* = 7 Hz, 3H). HRMS (ESI-TOF) *m/z* 680.2730 (calcd for C₃₆H₄₂NO₁₂ [M-H]⁻: 680.2707).

X-ray crystallography of 24-desmethylrifamycin S - Diffraction intensities were collected at 173(2) K on a Bruker Apex CCD diffractometer using MoK radiation = 0.71073 Å. Space group was determined based on systematic absences. Absorption corrections were applied by SADABS (33). Structures were solved by direct methods and Fourier techniques and refined on *F*² using full matrix least-squares procedures. All non-H atoms were refined with anisotropic thermal parameters. H atoms were treated in calculated positions in a rigid group model. It was found that solvent water is partially occupied in a position between molecules with an occupation factor of 0.25. H atoms in this solvent water molecule were not taken in consideration. The Flack parameter is 0.00(10). The relatively high value of *R*_{int}, 0.1271, is related to the fact that diffraction at high angles was very weak and intensity statistics at high angles are poor. All calculations were performed by the Bruker SHELXTL (v. 6.10) package (34). The crystal structure data for 24-desmethylrifamycin S (Table 1) has been deposited at the Cambridge Crystallographic Data Centre (deposition number: CCDC 1000828).

Synthesis of 24-desmethylrifampicin - 24-desmethylrifamycin S (5 mg, 0.0073 mmol) was dissolved in DMF (200 μL) and acetic acid (50 μL). After stirring the mixture at 50 °C, paraformaldehyde (3 mg) and 1,3,5-trimethyl-

hexahydro-1,3,5-triazine (8 μL) were added. The reaction was stirred at 50 °C for 2 h until all starting material was converted to 3-methyl-1,3-oxazino(5,6-c)-24-desmethylrifamycin, indicated by a blue spot on TLC. Subsequently, 1-amino-4-methyl-piperazine (8 μL) was added to the mixture. The reaction was stirred at the same temperature, and monitored by TLC until the disappearance of the blue spot and the formation of 24-desmethylrifampicin. The mixture was diluted with cooled 2% acetic acid (1.5 mL) and extracted three times with CHCl₃ (2 mL). The organic fractions were combined and concentrated to 1 mL and further washed 3 times with Brine solution. Organic fractions were combined and dried over anhydrous sodium sulfate then dried under a rotary evaporator. Crude fractions were subjected to silica gel chromatography with CHCl₃-MeOH in 10:1 and 8:1 ratio, as eluent. Fractions containing the product were pooled and further purified by HPLC [CH₃CN-0.05 M HCOONH₄ (60:40)] with (YMC-ODS-A, 250X10 mm ID, 5 microns particle size) column and flow rate 2 mL/min at 254 nm. Fractions containing 24-desmethylrifampicin were dried to afford the title compound (2.5 mg, 0.0031 mmol) of reddish orange powder. ¹H NMR (500 MHz, CD₃OD): HRMS (ESI-TOF) *m/z* 807.3829 (calcd for C₄₂H₅₅N₄O₁₂ [M-H]⁻: 807.3816).

Antibacterial assay - Antibacterial activity of rifampicin and its analogs were determined by agar diffusion assay. *Mycobacterium smegmatis* and *Staphylococcus aureus* were streaked on nutrient agar and incubated overnight at 37 °C. Colonies were transferred to nutrient broth and incubated at 37 °C for 24 h. The growth of the cultures was measured to a proper density at 600 nm (BioRad, SmartSpec 300). The inoculum (1 mL) was mixed thoroughly with warm nutrient agar (24 mL) and poured into petri dishes. The agar plates were allowed to solidify and dry for 30 min before assay. Sterile Whatman discs were impregnated with rifampicin and its analogs (20 μL) at a concentration of 1 mg/mL and dried at RT. The discs were placed onto inoculated agar plates and incubated at 37 °C for 24 h. To produce a contrast background of the inhibition zone, 0.25% MTT developing dye (2 mL) was added over the plates.

Drug sensitivity assays were done by Premas Biotech, Haryana, India, using various

concentrations of drugs (0.01 - 1 $\mu\text{g/ml}$). The drug testing was done using MB BacT/ALERT System (35), which is a mycobacterial detection system that utilizes a colorimetric sensor and reflectance detector to determine the level of carbon dioxide within the bottle. The bottle contains a medium and a MB/BacT reconstitution fluid, which promotes the growth of mycobacteria. As the bacteria grow, they produce CO_2 , which changes the color of the sensor located at the bottom of the bottle from green to yellow. The testing was performed with two controls: Direct growth control (DGC) and Proportionate growth control (PGC). DGC consists of 0.1 mL seed culture and 0.5 mL reconstitution fluid. PGC consists of 0.5 mL of DGC and 0.5 mL reconstitution fluid. Test bottle contains 0.5 mL seed culture, 0.5 mL reconstitution fluid, and the antibiotic. The test is considered as complete when the PGC bottle flags positive.

RESULTS

AT6 domain substitution in A. mediterranei S699 - It has been reported that the formation of naphthalene moiety in rifamycin biosynthesis occurs during chain elongation, specifically on module 4, as opposed to a result of a post PKS modification process (8,28,36). This reaction is catalyzed by *Rif-Orf19*, a 3-(3-hydroxyphenyl) propionate hydroxylase-like protein, which introduces a hydroxy group into the acyl carrier protein (ACP)-bound tetraketide and sets the stage for a cyclization reaction to form the naphthalene ring (28). Based on this, we designed a strategy to construct mutant strains of *A. mediterranei* S699 that might produce new rifamycin analogs, in which modification of the polyketide backbone occurs after the naphthalene ring formation (Fig. 2). We replaced the AT domain of module 6 (AT6) of the *rifPKS* (recognizes methylmalonyl-CoA as substrate) with the AT domain of module 2 (AT2) of the rapamycin PKS (recognizes malonyl-CoA) (Fig. 3A and Supplemental Fig. S1). For this purpose, the *rapAT2* domain excised from pMO2 (12), was sandwiched between PCR-I and PCR-II, 1.68kb and 1.5 kb DNA regions upstream and downstream of the AT6 domain of *rifPKS*, respectively. The resulting cassette (PCR-I/*rapAT2*/PCR-II) was then introduced into the vector pIJ4026 to give pAT6F (Fig. 3B). This non-replicative plasmid (containing erythromycin

resistance gene *ermE*) was electroporated into *A. mediterranei* S699 and the transformants were selected under erythromycin pressure.

Screening of first homologous recombinants yielded four single crossover (SCO) clones, which did not produce rifamycin, as indicated by the lack of brown pigmentation even after three weeks of incubation on agar plates (Supplemental Fig. S5A-D). Southern blot hybridization of their genomic DNA using [α - ^{32}P]-labeled pIJ4026 as probe confirmed the integration of PCR-I/*rapAT2*/PCR-II cassette in the chromosome (Supplemental Fig. S6A). The mutants were then grown on agar plates without antibiotic pressure for 3-4 generations to allow a second homologous recombination to occur. Screening of the colonies yielded three positive double crossover (DCO) clones, which were sensitive to erythromycin and produced brown pigmentation (Supplemental Fig. S5E-G). These clones were confirmed by Southern blot hybridization using DIG labeled *rapAT2* (Supplemental Fig. S6B). The DCO clones were also confirmed using PCR amplification and sequencing (data not shown). The *rapAT2* amplicons from these DCOs were identical to the *rapPKS* from *Streptomyces hygroscopicus*, indicating that the *rapAT2* domain has successfully replaced the *rifAT6* domain in *A. mediterranei* S699.

Production of rifamycin analogs by rifAT6::rapAT2 mutant - To investigate if the *rifAT6::rapAT2* mutant could produce rifamycin analogs, the wild-type and the mutant strains of *A. mediterranei* were grown in YMG medium (50 mL) for 7 days. The cultures were centrifuged and the supernatants were fractionated with ethyl acetate and analyzed by electrospray ionization mass spectrometry (Thermo Finnigan liquid chromatograph-ion trap mass spectrophotometer). Whereas the wild-type produced rifamycin B and rifamycin SV, the mutants produced compounds that gave *quasi*-molecular ions of m/z 740 and 682, which were 14 atomic mass units (amu) less than those of rifamycin B (m/z 754 [M-H] $^-$) and rifamycin SV (m/z 696 [M-H] $^-$), respectively (Fig. 4A-B). The results were consistent with the expected molecular masses for desmethyl analogs of rifamycin B and SV, although on the basis of these data alone it was not clear if the missing methyl group occurred at the expected C-24 position of the polyketide backbone.

Structure determination of 24-desmethylrifamycin B and 24-desmethylrifamycin SV - To confirm the chemical structure of the products, a 1 L scale culture of *rifAT6::rapAT2* mutant was prepared. The culture was extracted with EtOAc and the extract was subjected to SiO₂ column chromatography and HPLC (YMC C₁₈ 250 x 10 mm 5 micron, acetonitrile-0.5 M aq. ammonium formate 40:60, flow rate 2 mL/min, 254 nm). The major product (m/z 740 [M-H]⁻) was isolated (yield, 20 mg/L) and analyzed by ¹H and ¹³C NMR. The ¹H NMR spectrum of the compound revealed the presence of three pendant methyl groups [δ 0.72 (d, J = 6.5 Hz, 3H), 0.85 (d, J = 7 Hz, 3H), 0.92 (d, J = 6.5 Hz, 3H)], instead of four in rifamycin B [δ -0.30 (d, J = 4.5 Hz, 3H), 0.57 (d, J = 6 Hz, 3H), 0.97 (d, J = 6 Hz, 6H)], confirming the lack of a pendant methyl group in the mutant product (Fig. 4C-D). This is consistent with the expected product 24-desmethylrifamycin B. Interestingly, 24-desmethylrifamycin B is chemically rather unstable and can partially convert to 24-desmethylrifamycin SV and S in MeOH. ¹H NMR analyses of the latter compounds revealed the lack of signals for the glycolate moiety (Supplemental Fig. S7- S9).

Conversion of 24-desmethylrifamycin B to 24-desmethylrifamycin S - To further confirm the chemical structure of the products, 24-desmethylrifamycin B was oxidized to 24-desmethylrifamycin S using CuCl₂ as catalyst. The product was analyzed by (-)-ESI-MS (m/z of 680 [M-H]⁻, indicating the lack of the glycolate moiety and the presence of a naphthoquinone unit in the molecule) and ¹H NMR spectrum. Interestingly, during storage in CD₃OD at -20 °C, transparent red brown orthorhombic crystals were formed. These crystals were washed with cooled *n*-hexane and subsequently subjected to X-ray crystallographic analysis. The crystal structures revealed a dimeric form of 24-desmethylrifamycin S coordinating with Ca²⁺ through C-1, C-8, C-21, and C-23 oxygen atoms (Fig. 5). The results unambiguously confirmed the identity of the compound as 24-desmethylrifamycin S.

Synthesis of 24-desmethylrifampicin - To compare the biological activity of the new compound with the clinically used rifampicin, 24-desmethylrifamycin S was converted to 24-desmethylrifampicin by chemical synthesis. The synthesis was carried out according to the

published method for the preparation of rifampicin (37). Thus, treatment of 24-desmethylrifamycin S with paraformaldehyde and 1,3,5-trimethyl-hexahydro-1,3,5-triazine in the presence of acetic acid gave 3-methyl-1,3-oxazino(5,6-c)-24-desmethylrifamycin (Fig. 6). The product was then treated with 1-amino-4-methylpiperazine to give 24-desmethylrifampicin. Despite high purity of the product, as determined by TLC, HPLC, and ESI-MS (Supplemental Fig. S10 and S11), we were not able to obtain good quality NMR spectra of 24-desmethylrifampicin. This quandary might have been due to either partial oxidation of hydroquinone to quinone or reversible conformational changes of the compound that led to more than one conformer in the solution. However, attempts to improve the quality of the ¹H NMR spectrum by adding a trace amount of the reducing agent ascorbic acid, which is commonly used to reduce quinone to hydroquinone forms of rifamycin, or increasing the temperature during ¹H NMR measurements were unsuccessful. To confirm the utility of the synthetic method, we employed the same method to convert rifamycin S to rifampicin. The later compound gave an excellent ¹H NMR spectrum, identical to that of commercially available rifampicin (Supplemental Fig. S12). As there is no indication of quinone formation in rifampicin, it is predicted that the reversible conformational changes of 24-desmethylrifampicin is a more likely scenario. Nevertheless, to validate the identity of 24-desmethylrifampicin, a comparative MS/MS analysis was carried out (Supplemental Fig. S13). The result showed that 24-desmethylrifampicin (m/z 807 → 676 → 616 → 490 → 420) and rifampicin (m/z 821 → 690 → 630 → 490 → 420) have identical fragmentation patterns, albeit most of the fragments of 24-desmethylrifampicin are 14 atomic mass units less than the corresponding fragments from rifampicin (Supplemental Figs. S13 and S14). These fragmentation patterns are also consistent with those previously reported for rifampicin (38).

Antibacterial activity of 24-desmethylrifamycin S and 24-desmethylrifampicin - An antibacterial assay was carried out using 24-desmethylrifampicin, 24-desmethylrifamycin S and commercially available rifampicin and rifamycin S against *Mycobacterium smegmatis* and *Staphylococcus aureus*. The results showed

that 24-desmethylrifamycin S and 24-desmethylrifampicin are active against *M. smegmatis* and *S. aureus*, comparable to rifamycin S and rifampicin, respectively (Supplemental Fig. S15). This prompted us to carry on the study using multidrug resistant strains of *M. tuberculosis*. For this, MDR strains were procured from Open Source Drug Discovery (OSDD) (www.osdd.net/) and the drug testing was performed at Premas Biotech, Haryana, India, according to WHO guidelines. The drug sensitivity tests were carried out against two rifampicin-sensitive (OSDD 209 and H37Rv) and three rifamycin-resistant (OSDD 55, OSDD 206, and OSDD 321) strains of *M. tuberculosis* (Table 2). Rifampicin (HiMedia), 24-desmethylrifampicin and 24-desmethylrifamycin S were tested against the above-mentioned pathogenic strains. The tests were done at various concentrations (0.01 – 50 µg/mL) of drugs using BacT/ALERT MB System (35). The results revealed that 24-desmethylrifamycin S and 24-desmethylrifampicin showed strong antibacterial activity against both rifampicin-sensitive and -resistant strains of *M. tuberculosis*.

DISCUSSION

Although many derivatives of rifamycin have been synthesized by chemical methods in the past 40 years (39), only a handful of rifamycin derivatives are currently used for treating tuberculosis. Most rifamycin derivatives, including those used in the clinics, are chemically modified at the C-3 and/or the C-4 positions of the naphthalene moiety. Chemical modifications of other parts of the compound appear to be difficult to achieve due to the complexity of the molecule. In addition, X-ray crystallography studies of *Thermus aquaticus* RNAP complexed with rifampicin revealed that the four free hydroxy groups in the molecule are important for RNAP binding (2). Consequently, modifications of these hydroxyl groups are undesirable. Thus, this work focuses on the design of a strategy that gains access to rifamycin analogs, in which modifications take place in the polyketide backbone.

However, many complex polyketide systems similar to *rif*PKS have been reported to be less amendable to pathway engineering, either due to inflexibility of the downstream enzymes to accept modified substrates, or incompatibility in

architectural modularity of the modified PKS systems (40). Therefore, efforts to genetically engineer the *rif*PKS of *A. mediterranei* S699 were a somewhat risky and challenging endeavor. Additionally, the post PKS tailoring processes in rifamycin biosynthesis involving cytochrome P450-dependent hydroxylation and oxidative cleavage and rearrangement of the ansa chain (28,41) further augment the degree of complications in rifamycin biosynthesis. However, the most challenging aspect in the current study was the construction of the mutant strains of *A. mediterranei* S699. Gene transfer into this strain has so far only been successful through electroporation with undesirably low efficiency (28,29).

Nevertheless, the consideration of the formation of the naphthaquinone ring, which takes place during polyketide chain elongation (8,28), let us to target the replacement of the *rif*AT6 domain with that of *rap*AT2. Using this domain-replacement strategy, we successfully demonstrated that the *rif*PKS gene cluster is amendable to genetic manipulations and the mutants (*rif*AT6::*rap*AT2) can produce new rifamycin analogs, 24-desmethylrifamycin B and 24-desmethylrifamycin SV. While not completely unexpected, it is rather surprising that this complex biosynthetic system is adaptable to such a modification. However, whether this approach is applicable to the other *rif*PKS modules remains to be explored. More importantly, their semi-synthetic product, 24-desmethylrifampicin, showed comparable or better antibacterial activity than the clinically used rifampicin against various pathogenic bacteria, including rifampicin-sensitive and -resistant *M. tuberculosis*. This finding is significant because such a compound may be developed as a promising lead to cure MDR-TB.

Rifamycin resistance is associated with genetic alterations in an 81-bp region of the *rpoB* gene encoding the DNA-dependent RNAP β -subunit (42). In this study, we used rifampicin-resistant *M. tuberculosis* strains, OSDD 321 and OSDD 206, which contain the S531L mutation, and OSDD 55, which has the H526T mutation in the RNAP β -subunit. These mutations appear to alter the affinity of the RNAPs to rifampicin. In addition, on the basis of the reported crystal structures of bacterial RNAPs complexed with rifampicin (2), and the sequence data for

rifampicin-resistant RNAPs (42), we hypothesize that drug resistant mutations disrupt hydrogen bonding in the polyketide ansa chain. This was in part confirmed by the fact that 24-desmethylrifampicin showed improved activity against rifampicin-resistant *M. tuberculosis*. The loss of the methyl group in this compound is postulated to lead to conformational changes in the ansa chain that allow for more flexibility of the compound to bind mutated RNAPs. This conceivable conformational flexibility may be connected to the unsettled ^1H and ^{13}C NMR spectra of 24-desmethylrifampicin.

While 24-desmethylrifampicin showed improved efficacy against *M. tuberculosis*, compared to rifampicin it presents only a small structural change. Therefore, it is possible that resistant strains to 24-desmethylrifamycin can quickly develop. However, interestingly, even among the clinically used rifamycin derivatives, the tendency of bacterial resistance to those drugs is significantly different. For example, although rifampicin resistant strains of *M. tuberculosis* are now emerging, resistance to rifabutin has yet to be widely seen. In fact, some bacterial strains that confer resistance to rifampicin are still susceptible to rifabutin. X-ray crystal structural studies of the *T. thermophilus* RNAP in complex with rifapentin or rifabutin revealed additional interactions between their C-3/C-4 side chains and the enzyme (43). A more recent study on the crystal structures of the *E. coli* RNAP complexes with benzoxazinorifamycins has also demonstrated the role of the C-3/C-4 side chains in their improved binding to the protein (44). In the case of 24-desmethylrifamycin, we anticipate that conformational flexibility of the ansa chain may provide some advantages against mutated RNAPs. This may be further improved by chemical modifications of the C-3/C-4 positions of the compound, *e.g.*, adding benzoxazine moiety or other side chains, which can be effectively done by semi-synthesis using the mutant product as a scaffold.

Currently, the *rifAT6::rapAT2* mutant produces about 20 mg/L 24-desmethylrifamycin B, which is lower than the yield of rifamycin B produced by the wild-type strain S699 (50-100 mg/L). This is consistent with the common phenomenon observed in many genetically engineered strains, which often produce

combinatorial products in lower yields than the natural product (45). However, the yield may be increased through a classical strain improvement program, or by adopting the PKS domain replacement strategy to modify industrial strains, which can produce rifamycin B up to 24 g/L (21).

Furthermore, it is desirable to successfully apply the ‘proof-of-concept’ methodology developed in this study to further garner new rifamycin analogs by modifying its polyketide backbone. This may include replacement of the AT domains of other modules (loss or gain of a methyl group at other C-positions), inactivation of a dehydratase domain (introduction of an additional hydroxyl group) or a ketoreductase domain (introduction of a ketone). In addition, double or multiple modifications may also be pursued to generate more diverse analogs of rifamycin. Whereas effective strategies to achieve multiple genetic modifications still have yet to be developed, the combined genetic-synthetic approach applied in this study holds great potential to generate more rifamycin analogs to combat the threat of MDR strains of *M. tuberculosis* and/or other life-threatening pathogens.

REFERENCES

1. Hartmann, G. J., Heinrich, P., Kollenda, M. C., Skrobranek, B., Tropschug, M., and Weiss, W. (1985) Molecular mechanism of action of the antibiotic rifampicin. *Angew. Chem. Int. Ed. Engl.* **24**, 1009-1074
2. Campbell, E. A., Korzheva, N., Mustaev, A., Murakami, K., Nair, S., Goldfarb, A., and Darst, S. A. (2001) Structural mechanism for rifampicin inhibition of bacterial rna polymerase. *Cell* **104**, 901-912
3. August, P. R., Tang, L., Yoon, Y. J., Ning, S., Muller, R., Yu, T. W., Taylor, M., Hoffmann, D., Kim, C. G., Zhang, X., Hutchinson, C. R., and Floss, H. G. (1998) Biosynthesis of the ansamycin antibiotic rifamycin: deductions from the molecular analysis of the rif biosynthetic gene cluster of *Amycolatopsis mediterranei* S699. *Chem. Biol.* **5**, 69-79
4. Verma, M., Kaur, J., Kumar, M., Kumari, K., Saxena, A., Anand, S., Nigam, A., Ravi, V., Raghuvanshi, S., Khurana, P., Tyagi, A. K., Khurana, J. P., and Lal, R. (2011) Whole genome sequence of the rifamycin B-producing strain *Amycolatopsis mediterranei* S699. *J. Bacteriol.* **193**, 5562-5563
5. Schupp, T., Toupet, C., Engel, N., and Goff, S. (1998) Cloning and sequence analysis of the putative rifamycin polyketide synthase gene cluster from *Amycolatopsis mediterranei*. *FEMS Microbiol Lett* **159**, 201-207
6. Admiraal, S. J., Walsh, C. T., and Khosla, C. (2001) The loading module of rifamycin synthetase is an adenylation-thiolation didomain with substrate tolerance for substituted benzoates. *Biochemistry* **40**, 6116-6123
7. Admiraal, S. J., Khosla, C., and Walsh, C. T. (2003) A Switch for the transfer of substrate between nonribosomal peptide and polyketide modules of the rifamycin synthetase assembly line. *J. Am. Chem. Soc.* **125**, 13664-13665
8. Yu, T. W., Shen, Y., Doi-Katayama, Y., Tang, L., Park, C., Moore, B. S., Richard Hutchinson, C., and Floss, H. G. (1999) Direct evidence that the rifamycin polyketide synthase assembles polyketide chains processively. *Proc. Natl. Acad. Sci. U.S.A.* **96**, 9051-9056
9. Gaisser, S., Bohm, G. A., Cortes, J., and Leadlay, P. F. (1997) Analysis of seven genes from the eryAI-eryK region of the erythromycin biosynthetic gene cluster in *Saccharopolyspora erythraea*. *Mol. Gen. Genet.* **256**, 239-251
10. Schwecke, T., Aparicio, J. F., Molnar, I., Konig, A., Khaw, L. E., Haydock, S. F., Oliynyk, M., Caffrey, P., Cortes, J., Lester, J. B., and et al. (1995) The biosynthetic gene cluster for the polyketide immunosuppressant rapamycin. *Proc. Natl. Acad. Sci. U.S.A.* **92**, 7839-7843
11. Staunton, J., and Weissman, K. J. (2001) Polyketide biosynthesis: a millennium review. *Nat. Prod. Rep.* **18**, 380-416

12. Oliynyk, M., Brown, M. J., Cortes, J., Staunton, J., and Leadlay, P. F. (1996) A hybrid modular polyketide synthase obtained by domain swapping. *Chem. Biol.* **3**, 833-839
13. Jacobsen, J. R., Keatinge-Clay, A. T., Cane, D. E., and Khosla, C. (1998) Precursor-directed biosynthesis of 12-ethyl erythromycin. *Bioorg. Med. Chem.* **6**, 1171-1177
14. Xue, Q., Ashley, G., Hutchinson, C. R., and Santi, D. V. (1999) A multiplasmid approach to preparing large libraries of polyketides. *Proc. Natl. Acad. Sci. U.S.A.* **96**, 11740-11745
15. Ranganathan, A., Timoney, M., Bycroft, M., Cortes, J., Thomas, I. P., Wilkinson, B., Kellenberger, L., Hanefeld, U., Galloway, I. S., Staunton, J., and Leadlay, P. F. (1999) Knowledge-based design of bimodular and trimodular polyketide synthases based on domain and module swaps: a route to simple statin analogues. *Chem. Biol.* **6**, 731-741
16. Ruan, X., Pereda, A., Stassi, D. L., Zeidner, D., Summers, R. G., Jackson, M., Shivakumar, A., Kakavas, S., Staver, M. J., Donadio, S., and Katz, L. (1997) Acyltransferase domain substitutions in erythromycin polyketide synthase yield novel erythromycin derivatives. *J. Bacteriol.* **179**, 6416-6425
17. Lau, J., Fu, H., Cane, D. E., and Khosla, C. (1999) Dissecting the role of acyltransferase domains of modular polyketide synthases in the choice and stereochemical fate of extender units. *Biochemistry* **38**, 1643-1651
18. Stassi, D. L., Kakavas, S. J., Reynolds, K. A., Gunawardana, G., Swanson, S., Zeidner, D., Jackson, M., Liu, H., Buko, A., and Katz, L. (1998) Ethyl-substituted erythromycin derivatives produced by directed metabolic engineering. *Proc. Natl. Acad. Sci. U.S.A.* **95**, 7305-7309
19. Lal, R., Lal, S., Grund, E., and Eichenlaub, R. (1991) Construction of a hybrid plasmid capable of replication in *Amycolatopsis mediterranei*. *Appl. Environ. Microbiol.* **57**, 665-671
20. Lal, R., and Lal, S. (1994) Recent trends in rifamycin research. *Bioessays* **16**, 211-216
21. Lal, R., Khanna, M., Kaur, H., Srivastava, N., Tripathi, K. K., and Lal, S. (1995) Rifamycins: strain improvement program. *Crit. Rev. Microbiol.* **21**, 19-30
22. Lal, R., Khanna, R., Kaur, H., Khanna, M., Dhingra, N., Lal, S., Gartemann, K. H., Eichenlaub, R., and Ghosh, P. K. (1996) Engineering antibiotic producers to overcome the limitations of classical strain improvement programs. *Crit. Rev. Microbiol.* **22**, 201-255
23. Lal, R., Khanna, R., Dhingra, N., Khanna, M., and Lal, S. (1998) Development of an improved cloning vector and transformation system in *Amycolatopsis mediterranei* (*Nocardia mediterranei*). *J. Antibiot. (Tokyo)* **51**, 161-169
24. Khanna, M., Dua, M., and Lal, R. (1998) Selection of suitable marker genes for the development of cloning vectors and electroporation in different strains of *Amycolatopsis mediterranei*. *Microbiol. Res.* **153**, 205-211

25. Tuteja, D., Dua, M., Khanna, R., Dhingra, N., Khanna, M., Kaur, H., Saxena, D. M., and Lal, R. (2000) The importance of homologous recombination in the generation of large deletions in hybrid plasmids in *Amycolatopsis mediterranei*. *Plasmid* **43**, 1-11
26. Lal, R., Kumari, R., Kaur, H., Khanna, R., Dhingra, N., and Tuteja, D. (2000) Regulation and manipulation of the gene clusters encoding type-I PKSs. *Trends Biotechnol.* **18**, 264-274
27. Lal, R. (1999) Cloning vector and the process for the preparation thereof. in *US00598560A* (Patent, U. S. ed.)
28. Xu, J., Wan, E., Kim, C. J., Floss, H. G., and Mahmud, T. (2005) Identification of Tailoring Genes Involved in the Modification of the Polyketide Backbone of Rifamycin B by *Amycolatopsis mediterranei* S699. *Microbiology* **151**, 2515-2528
29. Xu, J., Mahmud, T., and Floss, H. G. (2003) Isolation and characterization of 27-O-demethylrifamycin SV methyltransferase provides new insights into the post-PKS modification steps during the biosynthesis of the antitubercular drug rifamycin B by *Amycolatopsis mediterranei* S699. *Arch. Biochem. Biophys.* **411**, 277-288
30. Kim, C. G., Yu, T. W., Fryhle, C. B., Handa, S., and Floss, H. G. (1998) 3-Amino-5-hydroxybenzoic acid synthase, the terminal enzyme in the formation of the precursor of mC7N units in rifamycin and related antibiotics. *J. Biol. Chem.* **273**, 6030-6040
31. Kaur, H., Cortes, J., Leadlay, P., and Lal, R. (2001) Cloning and partial characterization of the putative rifamycin biosynthetic gene cluster from the actinomycete *Amycolatopsis mediterranei* DSM 46095. *Microbiol. Res.* **156**, 239-246
32. Kieser, T., Bibb, M. J., Buttner, M. J., Chater, K. F., and Hopwood, D. A. (2000) *Practical Streptomyces Genetics*, The John Innes Foundation, Norwich, England
33. Sheldrick, G. M. (1998) Bruker/Siemens Area Detector Absorption Correction Program. Bruker AXS, Madison, WI
34. SHELXTL-6.10. Program for Structure Solution, Refinement and Presentation. *BRUKER AXS Inc.*, 5465 East Cheryl Parkway, Madison, WI 53711-5373 USA
35. Crump, J. A., Morrissey, A. B., Ramadhani, H. O., Njau, B. N., Maro, V. P., and Reller, L. B. (2011) Controlled comparison of BacT/Alert MB system, manual Myco/F lytic procedure, and isolator 10 system for diagnosis of *Mycobacterium tuberculosis* Bacteremia. *J. Clin. Microbiol.* **49**, 3054-3057
36. Stratmann, A., Toupet, C., Schilling, W., Traber, R., Oberer, L., and Schupp, T. (1999) Intermediates of rifamycin polyketide synthase produced by an *Amycolatopsis mediterranei* mutant with inactivated rifF gene. *Microbiology* **145** (Pt 12), 3365-3375
37. Marsili, L., and Pasqualucci, C. R. (1984) Process for the preparation of 3-iminomethyl derivatives of rifamycin SV. (Patent, U. S. ed., Gruppo Lepetit S.p.A, Italy)

38. Prasad, B., and Singh, S. (2009) In vitro and in vivo investigation of metabolic fate of rifampicin using an optimized sample preparation approach and modern tools of liquid chromatography-mass spectrometry. *J. Pharm. Biomed. Anal.* **50**, 475-490
39. Aristoff, P. A., Garcia, G. A., Kirchoff, P. D., and Hollis Showalter, H. D. (2010) Rifamycins--obstacles and opportunities. *Tuberculosis (Edinb)* **90**, 94-118
40. Khosla, C., Kapur, S., and Cane, D. E. (2009) Revisiting the modularity of modular polyketide synthases. *Curr. Opin. Chem. Biol.* **13**, 135-143
41. Wilson, M. C., Gulder, T. A., Mahmud, T., and Moore, B. S. (2010) Shared biosynthesis of the saliniketals and rifamycins in *Salinispora arenicola* is controlled by the sare1259-encoded cytochrome P450. *J. Am. Chem. Soc.* **132**, 12757-12765
42. Williams, D. L., Spring, L., Collins, L., Miller, L. P., Heifets, L. B., Gangadharam, P. R., and Gillis, T. P. (1998) Contribution of rpoB mutations to development of rifamycin cross-resistance in *Mycobacterium tuberculosis*. *Antimicrob. Agents. Chemother.* **42**, 1853-1857
43. Artsimovitch, I., Vassilyeva, M. N., Svetlov, D., Svetlov, V., Perederina, A., Igarashi, N., Matsugaki, N., Wakatsuki, S., Tahirov, T. H., and Vassilyev, D. G. (2005) Allosteric modulation of the RNA polymerase catalytic reaction is an essential component of transcription control by rifamycins. *Cell* **122**, 351-363
44. Molodtsov, V., Nawarathne, I. N., Scharf, N. T., Kirchoff, P. D., Showalter, H. D., Garcia, G. A., and Murakami, K. S. (2013) X-ray crystal structures of the *Escherichia coli* RNA polymerase in complex with benzoxazinorifamycins. *J. Med. Chem.* **56**, 4758-4763
45. Floss, H. G. (2006) Combinatorial biosynthesis--potential and problems. *J. Biotechnol.* **124**, 242-257

Acknowledgements - The authors thank Jesus Cortes (Entrechem SL Oviedo, Spain) for his helpful advice during the course of the project. We also thank Kim Gratz for her comments and assistance in the preparation of this manuscript. The authors also acknowledge Sukanya Lal, Richie Khanna, Monisha Khanna, Nidhi Dhingra, Gauri Dhingra, Dipika Tuteja, Rekha Kumari, Swati Majumdar for their help in the work; Shalini Lal and Deeksha Lal for reading the manuscript.

FOOTNOTES

*The work at Delhi University was supported by grants from the Department of Biotechnology, Government of India and Grants from the University of Delhi, India. Drug sensitivity assays were done by Premas Biotech, Haryana, India. Work at Oregon State University was supported by an Exceptional Opportunity Grant from the MJ Murdock Charitable Trust and the Medical Research Foundation of Oregon. AN, AS, UM, PK, RK and PS gratefully acknowledge the Council of Scientific and Industrial Research and University Grants Commission for providing research fellowships. KHA thanks the Government of Libya for providing a scholarship.

¹Abbreviations used are: TB, tuberculosis; RNAPs, RNA polymerases; PKS, polyketide synthase; AHBA, 3-amino 5-hydroxybenzoic acid; *rif*, rifamycin; AT, acyl transferase; *ery*, erythromycin; *rap*, rapamycin; ESI, electrospray ionization; SCO, single cross over; DCO, double cross over; SADABS, Bruker/Siemens

area detector absorption and other corrections; GROMACS, Groningen machine for chemical simulations.

FIGURE LEGENDS

FIGURE 1. Chemical structures of rifamycin B, its semisynthetic derivatives, and rapamycin.

FIGURE 2. Genetic organization of polyketide synthase gene cluster of rifamycin B biosynthesis. The chain is assembled from a starter unit (AHBA), 2 acetate and 8 propionate extender units. *RifF* encodes an amide synthase, which catalyzes the cyclization of the polyketide backbone. Post PKS modification and cyclization of polyketide backbone eventually leads to the formation of rifamycin B.

FIGURE 3. Construction of AT6 mutant of *Amycolatopsis mediterranei* S699. **A.** Partial polyketide assembly lines in rifamycin and rapamycin biosynthesis. AT6 domain of rifamycin PKS adds propionate, whereas AT2 domain of rapamycin PKS adds acetate to the growing polyketide chains. Proansamycin X is a precursor of rifamycin B. **B.** Schematic overview of homologous recombination events postulated to occur in *A. mediterranei* S699 to give an AT6 mutant.

FIGURE 4. Mass spectrometry and NMR spectroscopy analyses of rifamycin B and 24-desmethylrifamycin B. **A.** (-)-ESI-MS analysis of ethyl acetate extract of the AT6 mutant strain of *A. mediterranei* S699 that shows prominent peaks at m/z 740 (desmethylrifamycin B) and 682 (desmethylrifamycin SV). **B.** (-)-ESI-MS analysis of ethyl acetate extract of the wild-type strain that shows prominent peaks at m/z 754 (rifamycin B) and 696 (rifamycin SV). **C.** Partial ^1H NMR spectrum of rifamycin B. **D.** Partial ^1H NMR spectrum of 24-desmethylrifamycin B. Red stars show the four pendant methyl group in rifamycin B and blue stars show three pendant methyl groups in 24-desmethylrifamycin B.

FIGURE 5. X-ray crystal structure of 24-desmethylrifamycin S dimer in complex with Ca^{2+} . Broad red arrows indicate the missing methyl groups.

FIGURE 6. Synthetic scheme for 24-desmethylrifampicin.

TABLE LEGENDS

Table 1. Crystal data and structure refinement for 24-desmethylrifamycin S.

Table 2. Drug sensitivity data for rifampicin-resistant and -susceptible strains of *Mycobacterium tuberculosis* (procured from OSDD) against commercially available rifampicin and the novel compounds 24-desmethylrifamycin S and 24-desmethylrifampicin.

Table 1. Crystal data and structure refinement for 24-desmethylrifamycin S.

Empirical formula	$C_{72}H_{81}CaN_2O_{24.50}$	
Formula weight	1406.47	
Temperature	173(2) K	
Wavelength	0.71073 Å	
Crystal system	Orthorhombic	
Space group	C222(1)	
Unit cell dimensions	a = 14.257(7) Å	a = 90°.
	b = 20.818(11) Å	b = 90°.
	c = 25.054(13) Å	g = 90°.
Volume	7436(7) Å ³	
Z	4	
Density (calculated)	1.256 Mg/m ³	
Absorption coefficient	0.162 mm ⁻¹	
F(000)	2972	
Crystal size	0.22 x 0.22 x 0.08 mm ³	
Theta range for data collection	1.73 to 25.00°.	
Index ranges	-16<=h<=16, -24<=k<=24, -29<=l<=29	
Reflections collected	35699	
Independent reflections	6539 [R(int) = 0.1271]	
Completeness to theta = 25.00°	100.0 %	
Absorption correction	Semi-empirical from equivalents	
Max. and min. transmission	0.9872 and 0.9653	
Refinement method	Full-matrix least-squares on F ²	
Data / restraints / parameters	6539 / 0 / 452	
Goodness-of-fit on F ²	1.059	
Final R indices [I>2sigma(I)]	R1 = 0.0924, wR2 = 0.2301	
R indices (all data)	R1 = 0.1322, wR2 = 0.2576	
Absolute structure parameter	0.00(10)	
Extinction coefficient	0.0048(6)	
Largest diff. peak and hole	1.090 and -0.483 e.Å ⁻³	

Table 2. Drug sensitivity data for rifampicin-resistant and -susceptible strains of *Mycobacterium tuberculosis* (procured from OSDD) against commercially available rifampicin and the novel compounds 24-desmethylrifamycin S and 24-desmethylrifampicin.

<i>M. tuberculosis</i> strain		rifampicin (HiMedia) (µg/ml)	24-desmethyl-rifamycin S (µg/ml)	24-desmethyl-rifampicin (µg/ml)
OSDD 55 (H526T)	Resistant	>50	0.1	<0.01
OSDD 206 (S531L)		>50	0.05	0.05
OSDD 321 (S531L)		>50	0.1	0.05
OSDD 209*	Susceptible	0.1	<0.01	<0.01
H37Rv*		0.05	<0.01	0.05

* no rpoB mutation

Figure 1

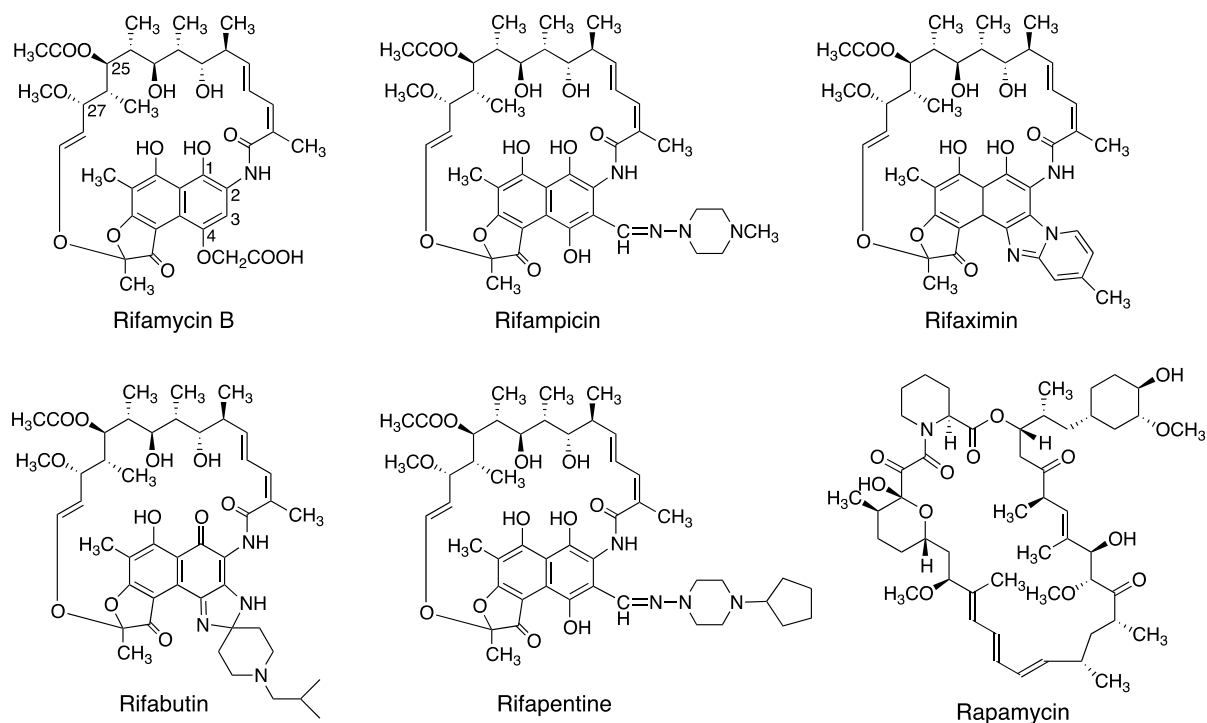


Figure 2

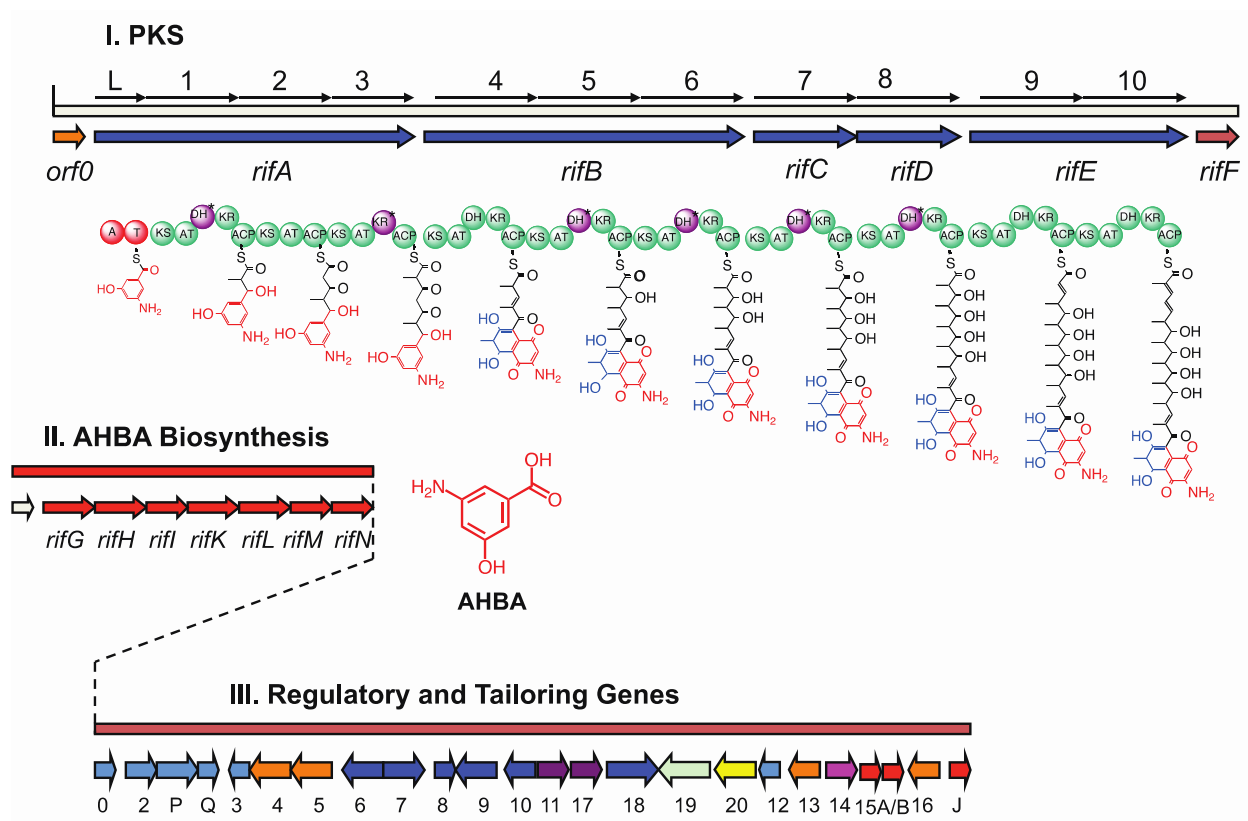


Figure 3

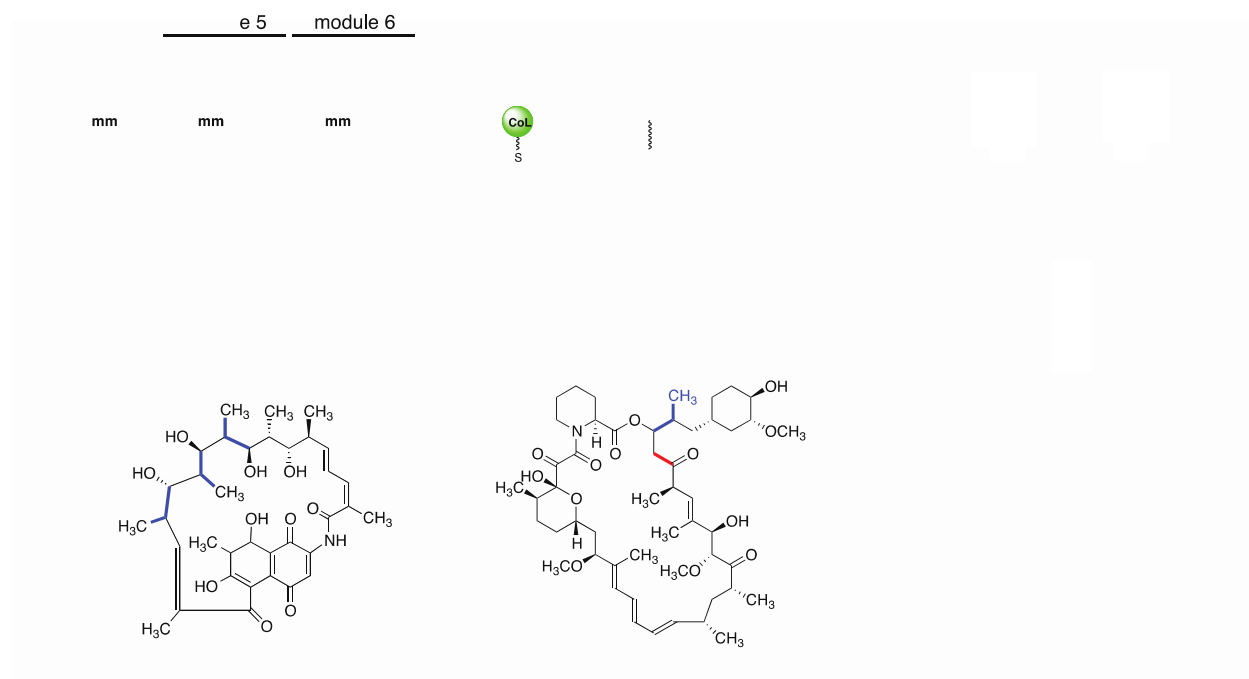
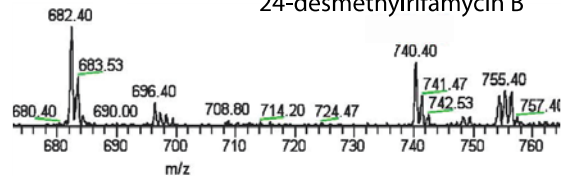


Figure 4

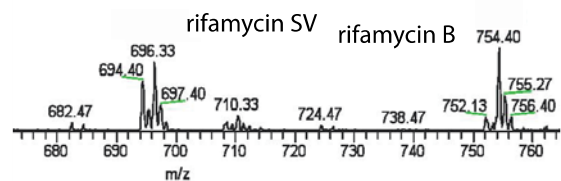


24-desmethylrifamycin SV

24-desmethylrifamycin B



rifamycin SV



rifamycin B

ylrifamycin B

Figure 5

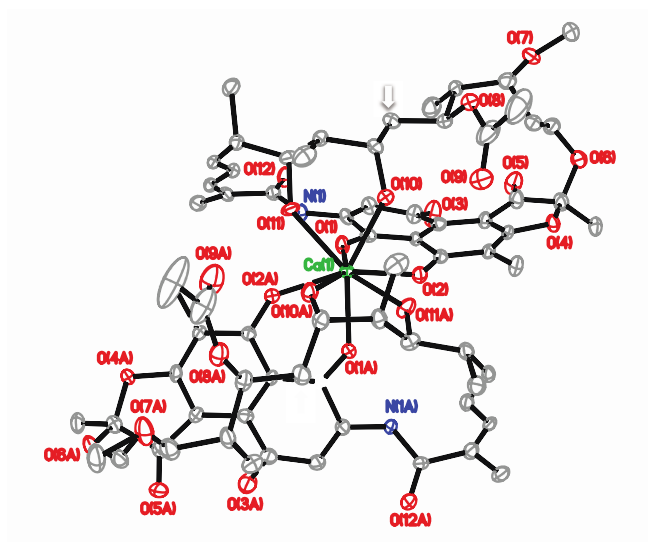


Figure 6

